Coherent emission of atomic soliton pairs by Feshbach-resonance tuning

Humberto Michinel,[1] Ángel Paredes,[1] María M. Valado,[2,3] and David Feijoo[1]

[1]*Área de Óptica, Facultade de Ciencias de Ourense, Universidade de Vigo, As Lagoas s/n, Ourense, ES-32004 Spain*
[2]*Dipartamento di Fisica "E. Fermi," Università di Pisa, Largo Pontecorvo 3, 56127 Pisa, Italy*
[3]*INO-CNR, Largo Pontecorvo 3, 56127 Pisa, Italy*

We present two simple designs of matter-wave beam splitters in a trapped Bose-Einstein condensate (BEC). In our scheme, identical pairs of atomic solitons are produced by an adequate control—in time and/or space—of the scattering length. Our analysis is performed by numerical integration of the Gross-Pitaevskii equation and supported by several analytical estimates. Our results show that these devices can be implemented in the frame of current BEC experiments. The system has potential applications for the construction of a soliton interferometer.

I. INTRODUCTION

One of the most promising research tracks in the field of Bose-Einstein condensation (BEC) in gases [1] is the design of interferometric devices using coherent matter waves [2,3]. The potential use of these novel atomic interferometers in new types of sensors [4], precision measurements [5], and in the study of gravitational effects [6], among other areas, has become a very active topic and different schemes have been proposed, most of them based on the control of the atomic cloud by time-dependent traps [7].

Although the general principles of interferometry apply to both coherent light and matter waves on equal footing, there are important distinctions between optical and atomic devices. Besides the different intrinsic nature of waves and the physical scales involved in both cases, one of the most remarkable gaps is that the design of accurate and controllable atomic beam splitters is much more difficult as compared to light systems—it must be said, though, that it is possible to implement atomic quantum interferometry without such a beam splitter [8]. Moreover, once a pair of BEC pulses is produced, the atomic clouds will show a significant spreading due to internal repulsive interactions. This dilution of the waves may diminish dramatically the signal-to noise ratio of the device, precluding the detection of the effects under study, especially if their traces are minimal as is the case of many gravitational and quantum interactions [9].

The use of atomic soliton sources [10,11], which produce self-trapped matter-wave packets that propagate undistorted, can be an interesting strategy to avoid the spreading and provide precision interferometric measurements. This possibility, already pointed out in Ref. [10], has been recently pursued in Refs. [12–18]. The engineering of a coherent soliton beam splitter by manipulations of the external potential [13,14,16–18] or by making use of a Rabi coupling between two atomic states of the particles in the sample [15] has been discussed.

The goal of this work is to introduce protocols for the control of atomic clouds that can coherently produce soliton pairs. The evolution is controlled by an appropriate tuning of the strength and sign of the interatomic interactions. Our construction is similar to the simple pulsed atomic soliton laser first proposed by Carr and Brand in Ref. [19], where simulations showed that a train of robust matter pulses can be generated by the mechanism of modulational instability (MI). However, the device of [19] has limited utility in the frame of interferometry due to the following drawbacks: (i) the number of wave packets generated cannot be controlled and they have different shapes; (ii) the trap must be destroyed after outcoupling; (iii) several pulses are always produced whereas in many applications single-pair sources are of interest; and (iv) the pulses will travel at different speeds once the trap is removed.

In the following, we will show a simple mechanism that allows the previous limitations to be overcome, yielding atomic coherent sources suitable for unusual types of matter-wave interferometers. This is interesting since the techniques for generating and controlling BECs with growing numbers of particles and their physical properties are nowadays well established, and the current experimental challenges in the field concern the design of practical devices [20].

Thus, in the present paper, we will demonstrate that pairs of counterpropagating atomic solitons can be emitted from a trapped BEC reservoir by an adequate tuning of the scattering length a. The idea is quite simple: if the atomic cloud is placed in the center of a shallow trap and a is tuned to a large positive value, the atomic cloud will spread due to strong internal repulsive interactions. When the width of the cloud is large enough, the interatomic forces are switched from repulsive to attractive by means of Feshbach-resonance tuning [21,22]. Then, modulational instability yields soliton formation [23]. Once the symmetric pair of solitons is produced, the matter-wave pulses leave the trap with opposite velocities. The key point is that *an adequate tuning of the scattering length allows full control over the splitting process*. We will show that this idea can be accomplished by modulating a either in time or in space.

An atomic Michelson interferometer configuration can be easily implemented by the addition of a wide parabolic potential that forces the solitons to return and interfere. As we will show in the rest of this work, this simple device can be straightforwardly built in the frame of current experiments with ultracold atoms.

II. SYSTEM CONFIGURATION AND MATHEMATICAL MODEL

For our analysis, we will assume a quasi-one-dimensional BEC, strongly trapped in the transverse directions (x,y) by a

parabolic trap $V_\perp$ of characteristic frequency $\omega_\perp$ and weakly confined in the longitudinal dimension (z) by a shallow optical-dipole trap with a Gaussian shape [24,25]. The choice of this geometry is justified by the need of outcoupling atoms along the z axis, so the strength of the atomic interactions may be tuned to overcome the shallow potential. Thus, the trap will have the following mathematical form:

$$V(\vec{r}) = V_\perp + V_d = \frac{m\omega_\perp^2}{2}(x^2 + y^2) + V_0\left[1 - \exp\left(-\frac{z^2}{L^2}\right)\right],$$
(1)

where m is the mass of the atoms, V_0 is the depth of the shallow optical-dipole potential, and L is its characteristic width. The well-known mean-field theory for a system of N equal bosons of mass m, weakly interacting in a potential, yields a Gross-Pitaevskii [26] equation (GPE) of the form

$$i\hbar\frac{\partial\Psi}{\partial t} = -\frac{\hbar^2}{2m}\nabla^2\Psi + V(\vec{r})\Psi + U(t,\vec{r})|\Psi|^2\Psi,$$
(2)

where Ψ is the condensate wave function and $N = \int|\Psi|^2 d^3\vec{r}$ the number of atoms. The coefficient $U(t,\vec{r}) = 4\pi\hbar^2 a(t,z)/m$ characterizes the two-body interaction which we consider a time- and space-dependent function. In this situation, we can describe the dynamics of the condensate in the quasi-one-dimensional limit as given by a factorized wave function of the form [27] $\Psi(t,\vec{r}) = e^{-i\omega_\perp t}\Phi_0(x,y)\psi(t,z)$, where $\Phi_0(x,y)$ is a Gaussian and $\psi(t,z)$ is determined by

$$i\frac{\partial\psi}{\partial\tau} = -\frac{1}{2}\frac{\partial^2\psi}{\partial\eta^2} + f(\eta)\psi + g(\tau,\eta)|\psi|^2\psi.$$
(3)

Our analysis is based on this equation. We have introduced the dimensionless variables

$$\tau = \omega_\perp t, \quad \eta = z/r_\perp = z/\sqrt{\hbar/m\omega_\perp},$$
(4)

which are the time measured in units of the inverse of the transverse trapping frequency and the length along the z axis expressed in units of $r_\perp$—which determines the size of the cloud in the transverse (x,y) plane. The functions

$$f(\eta) = \frac{V_d}{(\hbar\omega_\perp)}, \quad g(\tau,\eta) = \frac{2a(\tau,\eta)}{r_\perp}$$
(5)

correspond, respectively, to the trap and to the effective atomic interaction coefficient. We must stress that g depends on time and space and can be externally tuned; this is a key point of our analysis. The new normalization is $\int|\psi|^2 d\eta = N$.

The simulations and figures that follow have been made with standard experimental parameters corresponding to ^{7}Li atoms. In particular, we will take $\omega_\perp = 1$ kHz, and $r_\perp = 3$ μm. The choice of ^{7}Li has been motivated by previous well-known results on soliton formation [10,11]; however, we must stress that our results can be straightforwardly extrapolated to different values of $\omega_\perp$ and to other atomic species provided that external control of the scattering length can be achieved. Since our goal is to study manipulations via Feshbach-resonance tuning, we will also fix the parameters determining the external potential: $L = 15r_\perp$ and $V_0 = \hbar\omega_\perp/4$—in the following, we will also use the definitions $\tilde{L} = L/r_\perp$ and $\tilde{V}_0 = V_0/(\hbar\omega_\perp)$.

III. SOLITON-PAIR EMISSION WITH A TIME-DEPENDENT SCATTERING LENGTH

In Fig. 1 a numerical simulation of the effect of a sharp tuning with time of the scattering length a is shown. For $\tau < 0$, we have $a = a_i = L\tilde{V}_0\sqrt{\pi}/(2N)$, such that, in the Thomas-Fermi approximation, there is a stationary solution with a Gaussian shape. This provides an initial condition for the subsequent time evolution:

$$\psi(\tau = 0, \eta) = \frac{\sqrt{N}}{\pi^{1/4}\sqrt{\tilde{L}}}\exp\left(-\frac{\eta^2}{2\tilde{L}^2}\right)$$
(6)

The value of a is assumed to change at $\tau = 0$ to a larger one $a_1 > a_i$. Therefore, the strength of the repulsive atomic interactions will stretch the BEC wave function, as the shallow Gaussian potential is not strong enough to keep the cloud trapped. The broadening effect can be appreciated in the plots labeled (a) and (b) in the left column of Fig. 1. Once the cloud
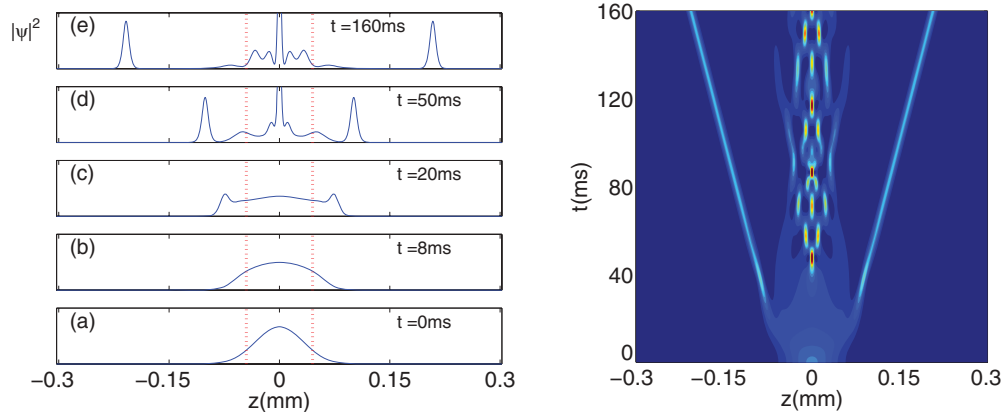
FIG. 1. (Color online) Simulation showing the controlled emission by sharp tuning of the scattering length of a trapped BEC, yielding a pair of equal counterpropagating solitons. The experimental parameters correspond to ^{7}Li atoms with $N = 5 \times 10^4$ and $a_i = 0.2$ nm. At $t = 0$, the scattering length is set to $a_1 = 1.5$ nm and at $t = t_s = 8$ ms, it is tuned to $a_2 = -0.2$ nm. Left: evolution of the wave function $|\psi|^2(z)$ at different times indicated in the plots. The red dotted lines indicate the size of the trap. Each of the two emitted solitons contains around 8500 atoms. Right: color contour map of the whole process.
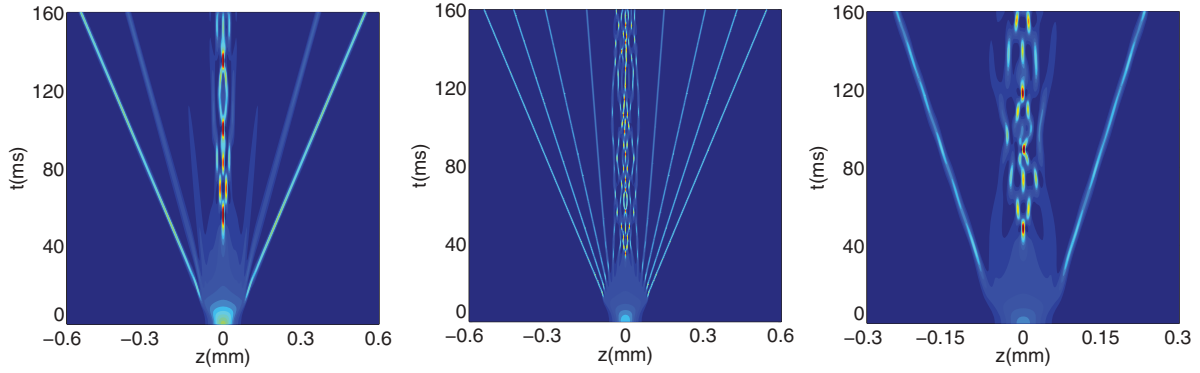
FIG. 2. (Color online) Emission of an increasing number of pulses by an adequate control of the value of a with time. In the first plot, we have taken $a_1 = 3$ nm, $a_2 = -0.2$ nm. In the second, $a_1 = 3$ nm, $a_2 = -1$ nm. The total number of atoms $N = 5 \times 10^4$ is as in Fig. 1. In the third plot, we repeat the simulation of Fig. 1 but allowing noise in the initial wave function. We have discretized the initial function ψ, performed a fast Fourier transform, and multiplied its value at each point by a real pseudorandom number obtained from a normal distribution with mean 1 and standard deviation 0.2. After time evolution, the outcome does not change substantially.

spreads out of the trap, the interactions are instantaneously switched to a negative value a_2 at $t = t_s$. This can be done with standard magnetic [21] or optical [22] techniques which allow the values of a to be tuned over a wide range. The effect on the cloud can be seen on Figs. 1(c) and 1(d). The modulational instability effect [19] in the stretched condensate yields solitons that move away with a constant velocity, as can be appreciated in the contour plot on the right side of the figure.

We must stress that not only one but a controllable number of soliton pairs can be produced by means of the technique proposed. This is shown in Fig. 2, where we illustrate the emission of an increasing number of pulses by an adequate control of the value of a with time. In the last plot of Fig. 2, we show that the process is not greatly modified in the presence of a limited amount of noise. We also stress that the production of pairs can be achieved for a wide range of values of the scattering lengths. These observations accentuate the robustness of the process.

Atomic Michelson interferometer. In Fig. 3 we show a simulation of a simple Michelson interferometer that can be easily implemented by simply adding a wide parabolic trap to the previous configuration, such that solitons eventually collide and yield an interference pattern [28]. In the absence of interaction of the soliton with the rest of the atoms the center

of mass of the soliton would behave as a classical particle in the external potential due to an Ehrenfest theorem—see, for instance, [29]. The time at which solitons meet and interfere would then be around $2\pi/\omega_z$. In the figures one can appreciate that the interference happens earlier because of the attractive interaction from the atoms in the trap. We also show that if a linear perturbation is added to the potential, it is possible to have the solitons interfering outside the Gaussian trap. In Fig. 4, we enlarge the interesting interference region.

Simple modelization. In order to give the experimentalists a brief guide and get a qualitative understanding of the physics, we can make a simple analysis of the process and give a rough approximation to the number of solitons produced as a function of the main physical parameters involved (N, a_1, a_2).

The first step of the process is the expansion due to large, positive a_1. We can find an estimate of the expansion rate by making use of the variational method called the averaged Lagrangian formalism [30]. We use the following variational ansatz:

$$\psi = A(\tau) e^{-\eta^2/2w(\tau)^2} e^{i[\mu(\tau)+\eta\,\alpha(\tau)+\eta^2\,\beta(\tau)]}, \qquad (7)$$

where $A(\tau)$, $w(\tau)$, $\mu(\tau)$, $\alpha(\tau)$, and $\beta(\tau)$ are real functions to be determined by minimizing the action from which GPE stems [30]. A straightforward analysis yields $\alpha(\tau) = 0$ as
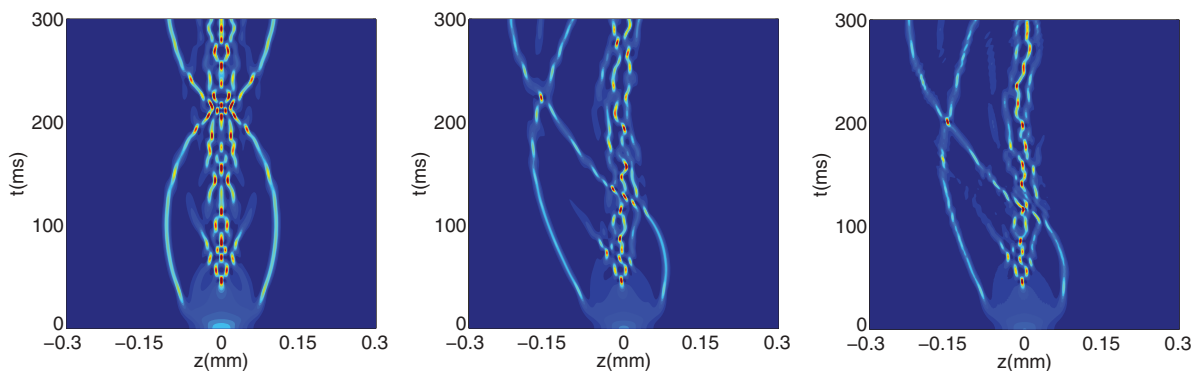
FIG. 3. (Color online) Simulation of a simple Michelson interferometer. The first plot is a simulation with a harmonic potential along the z axis, $\omega_z = 0.01\omega_\perp$. The rest of the parameters are as in Fig. 1. In the second plot we have added a small linear perturbation to V_d, namely, $0.0025\hbar\omega_\perp z/r_\perp$. The third plot is as the second one with noise included in the initial condition, as explained in the caption of Fig. 2.
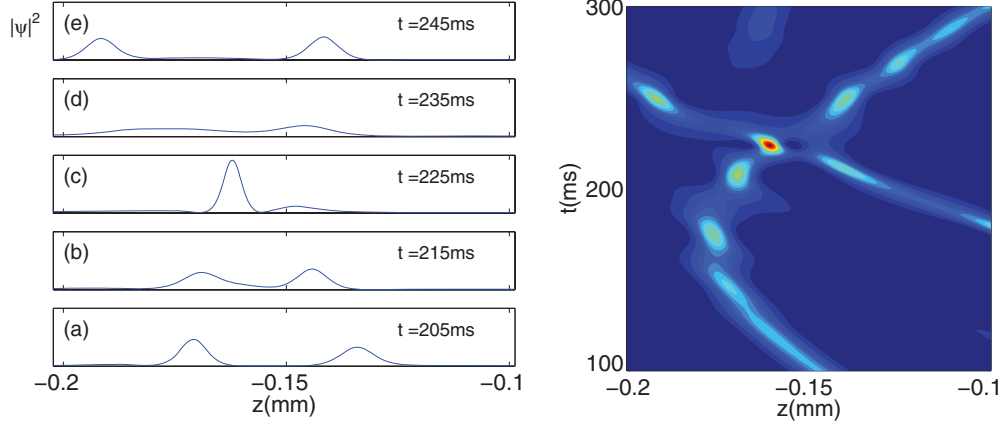
FIG. 4. (Color online) Enlargement of the second plot of Fig. 3 around the region where the solitons cross. Left: evolution of the wave function $|\psi|^2(z)$ at different times indicated in the plots. One can appreciate constructive-destructive interference when the solitons meet. Right: color contour map of the enlarged region.

implied by the $\eta \to -\eta$ symmetry of the problem, $A(\tau) = \frac{\sqrt{N}}{\pi^{1/4}\sqrt{w(\tau)}}$ as required by normalization, $\beta(\tau) = \frac{\dot{w}(\tau)}{2w(\tau)}$, a first-order ordinary differential equation (ODE) for $\mu(\tau)$ which we do not write, and

$$\ddot{w}(\tau) = -\frac{d\Pi}{dw(\tau)} \tag{8}$$

with the pseudopotential

$$\Pi = \frac{1}{2w(\tau)^2} + \tilde{L}\,\tilde{V}_0\left(\frac{g}{\sqrt{2}g_0 w(\tau)} - \frac{2}{\sqrt{\tilde{L}^2 + w(\tau)^2}}\right). \tag{9}$$

We ought to solve (8) with the initial conditions $w(0) = \tilde{L}$, $\dot{w}(0) = 0$. Noticing that $\frac{1}{2}\dot{w}^2 + \Pi$ is a conserved quantity, one can estimate the expansion velocity at the time when the scattering-length sign is swapped. Considering that the second term in (9) is the dominant one and assuming that the change in a is performed when $w \approx 2\tilde{L}$, we find $\dot{w}|_{\text{out}} \approx (2/\pi)^{1/4}\sqrt{a_1 N/L}$.

The second step of the process is soliton formation via modulational instability when the scattering length becomes $a_2 < 0$. For a flat initial wave function, there is a wavelength of the perturbation for which the instability is maximal [31], which, in terms of our dimension-less formalism, reads $l = 2\pi\sqrt{w/|g_2|N}$. The number of produced solitons is obtained by dividing the size of the wave function by this length. We should just consider the atoms which are outside the trap so they can escape. Thus, the relevant condensate size for soliton formation can be approximated by $2r_\perp(\dot{w}|_{\text{out}}\tau_s - \tilde{L})$. Putting everything together, we find the following expression for the functional dependence of the number of solitons in the adimensional parameters:

$$N_s \approx 2\left[\frac{c_1\sqrt{|g_2|N}(c_2\sqrt{g_1 N} - \tilde{L})}{(g_1 N)^{1/4}}\right]. \tag{10}$$

We have compared this estimate to the outcome of numerical simulations (keeping always $\tau_s = 8$, $\tilde{L} = 15$, $\tilde{V}_0 = 0.25$) and found that, introducing the fitted coefficients $c_1 = 0.22$ and $c_2 = 2.49$, Eq. (10) is a reasonably accurate approximation in a wide range of parameters; see Fig. 5. We have also confirmed by numerical simulations that the estimate for $\dot{w}|_{\text{out}}$ is related

to the velocity of the fastest outgoing soliton which turns out to grow—roughly—as $\sqrt{a_1 N}$.

IV. SOLITON-PAIR EMISSION WITH A SPACE-DEPENDENT SCATTERING LENGTH

We explore now a second possibility, and we consider an s-wave scattering length which varies in space. We will utilize

$$a(z) = a_2 + (a_1 - a_2)\exp(-z^2/L^2) \tag{11}$$

for $\tau > 0$. As before $a_1 > a_i > 0$, $a_2 < 0$. Since a is positive for small z, atoms are pushed out of the trap. The negative a for larger z contributes to this stretching process and, additionally, it can repack the outgoing atom cloud into solitons [32].
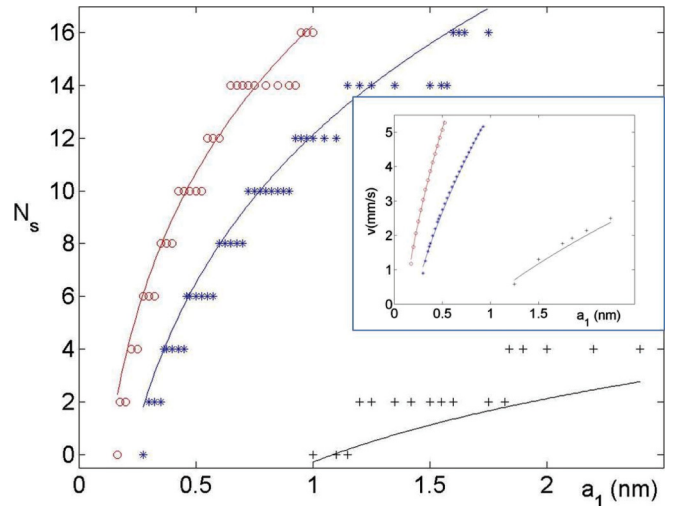
FIG. 5. (Color online) Some examples of comparison of the number of emitted solitons (as computed from numerical simulations) with the approximate expression (10) (solid lines). In each case we plot N_s vs a_1 for fixed N and a_2. The three curves, from top to bottom, correspond to $N = 4.5 \times 10^5$, $a_2 = -0.1$ nm; $N = 2.5 \times 10^5$, $a_2 = -0.2$ nm, and $N = 0.5 \times 10^5$, $a_2 = -0.2$ nm. In the inset, we compare the speed of the fastest emitted solitons to fits of the form $v \approx -b_1 + b_2\sqrt{a_1 N}$ in the same three cases.
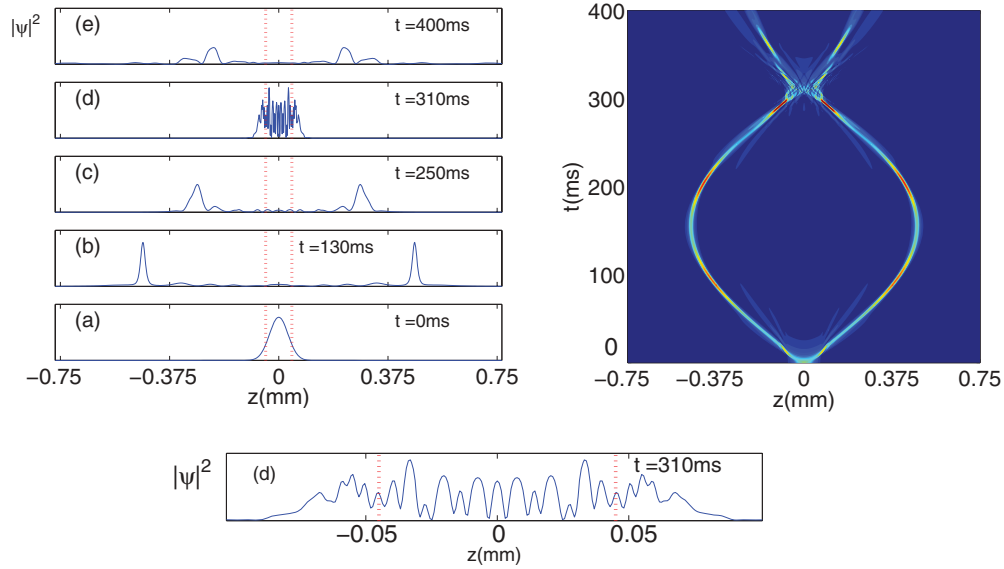
FIG. 6. (Color online) Emission and subsequent interference of a soliton pair with a space-varying s-wave scattering length, Eq. (11). We have taken $N = 3.5 \times 10^4$, $a_1 = 5$ nm, and $a_2 = -0.1$ nm. There is an external harmonic potential $\omega_z = 0.01\omega_\perp$. In the graph below, we show an enlargement of (d), exhibiting the interference pattern.

We show in Fig. 6 that, by appropriately tuning the physical parameters, it is possible to create a soliton pair while leaving the Gaussian trap almost empty. This can be an advantage as compared to Sec. III. As in the previous case, these solitons can be made to interfere by turning on a parabolic potential in the axial direction. It is worth noticing that, when the solitons reenter the small-z region, they disintegrate as they return to the region of positive a. The resulting atoms interfere yielding a typical pattern of fringes; see Fig. 6(d).

As an example, let us discuss an extremely simple interferometric Michelson-like gedanken experiment. We add a linear term to the external potential:

$$V_d = V_0 \left[1 - \exp\left(-\frac{z^2}{L^2} \right) \right] + \frac{1}{2} m \omega_z^2 z^2 + m \gamma z. \quad (12)$$

We assume that γ is tunable and that we wish to determine its value. The linear potential affects the soliton trajectories and causes a displacement of the fringe pattern. As in a typical optical Michelson experiment, the resolution of the interferometer should be related to the shift in γ that displaces one maximum of the interference pattern to the position of the next one. A convenient way to estimate this resolution from numerical simulations is to compute the atom density at the center of the trap when the interference takes place, say, at $t = t_m = 310$ ms and $z = 0$; see Fig. 7. Since it is the whole interference pattern being displaced, a similar plot would be found at any position z inside the trap.

The order of magnitude of the minimal acceleration that may be measured with such a device is related to the spacing between maxima in the plot, namely, $\gamma \approx 2 \times 10^{-4}$ m/s². We stress that this simple estimation is solely based on the computation of the displacement of the fringes. When, eventually, a method is put forward to measure the fringe displacement in an actual experimental setup, there may well be experimental considerations that could influence the resolution.

Let us now provide an analytical estimation of the value of γ found above. The difference in the paths of the two parts of the beam when the interference pattern is shifted by one maximum should be given by $\frac{mv\Delta z}{\hbar} = \pi$ where mv is the momentum when the atoms interfere. By considering the solitons as particles in a classical potential which depart initially from $z = 0$ with opposite velocities, one can check that the difference in their paths before meeting again is $\Delta z = 4\gamma/\omega_z^2$. In order to find a rough approximation to the momentum, we use the estimate of the previous section for the velocity of the outgoing solitons, which in terms of dimensionful quantities reads $v \approx (\frac{2}{\pi})^{1/4} \sqrt{\frac{a_1 N}{L}} r_\perp \omega_\perp$. Inserting
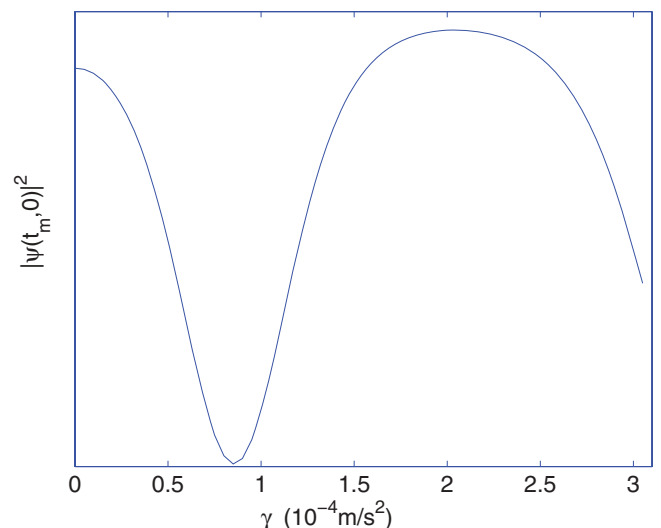
FIG. 7. (Color online) The value of the atom density (arbitrary units) at the center of the trap at time $t = 310$ ms, computed by numerical integration, as a function of the uniform acceleration γ caused by an external force.

these values of Δz and v in the condition above and inserting the value of the parameters used in Figs. 6 and 7, one finds $\gamma \approx \frac{\pi^{5/4}}{2^{9/4}} r_\perp \omega_z^2 \sqrt{\frac{L}{a_1 N}} \approx 1.3 \times 10^{-4}$ m/s^2, which captures the order of magnitude of the value obtained from the plot.

V. DISCUSSION

We have shown that, by an appropriate tuning in time and/or space of the *s*-wave scattering length related to the atom-atom interaction, it is possible to engineer a beam splitter for atomic interferometers. In particular, we have analyzed the possibility of generating a soliton pair. We emphasize that this can be done in a controlled way and in a broad regime of the physical parameters than can be typically achieved in BEC experiments. We have shown the results for a particular set of dimensionful parameters, but they can be easily generalized to different situations. It is reasonable to expect that the robustness and lack of dispersion involved in soliton propagation might prove useful in ameliorating the precision obtained in atom interferometers which deal with BECs but not with solitons. The next natural step is to design a concrete experiment to measure, for instance, the gravity acceleration g or to test gravity at short distances, but this lies beyond the scope of the present work.

Our analysis of the dynamics has been performed using a reduction to one dimension of the GPE, Eq. (3). This one-dimensional (1D) approximation remains sensible as long as the atoms are not energetic enough to get excited and probe the transverse directions. We now discuss in more detail the validity and limitations of Eq. (3). The first relevant issue is how good is the approximation leading to the reduction of Eq. (2) to its 1D counterpart Eq. (3). For a recent analysis, see [33]. Of particular importance is the fact that, with attractive interactions, collapses not describable with (3) may occur. Avoiding collapse in the transverse 2D space or collapse of a single soliton requires conditions [19] which in our notation read $-g|\psi|^2 < 0.93$ and $-g N_{\text{ais}} < 1.254$, where N_{ais} stands for the number of atoms in a soliton. These limitations have, in part, motivated our choice of physical parameters in the previous sections.

On the other hand, the GPE describes the evolution of a condensate at vanishing temperature. In any realistic situation, there will be corrections controlled by the adimensional quantity $\frac{k_B T}{\hbar \omega_\perp}$. The thermal cloud can produce friction for the motion of the soliton [34] or deplete the condensation and even cause incoherent splitting of a soliton after some time [35]. These considerations affect the coherent evolution of the system and therefore the sensibility of an eventual soliton interferometer will depend on the temperature of the atom cloud. It would be of great interest to explore this point.

Moreover, when one deals with elongated condensates, as is the case of this paper, one has to take into account that there may be non-negligible fluctuations of the phase along the axial direction, even well below the BEC transition temperature T_c [36]. The most important contributions come from fluctuations of wavelength larger than $r_\perp$, due to the similarity of the system to 1D trapped gases [37]. The equilibrium state is a *quasicondensate*. If these fluctuations were large, they would hinder any interferometric measurement so it is essential to estimate their amplitude. Using the Thomas-Fermi approximation for an elongated trap with repulsive interactions, in [36] it was shown that phase fluctuations are controlled by the parameter

$$\delta_L^2(T) = \frac{T}{T_c} \left(\frac{N}{N_0} \right)^{3/5} \delta_c^2, \tag{13}$$

where N is the total number of atoms in the sample, N_0 the number of those which are condensed, and

$$\delta_c^2 = \frac{16 a^{2/5} m^{1/5} \omega_\perp^{22/15}}{15^{3/5} N^{4/5} \hbar^{1/5} \omega_\parallel^{19/15}}, \tag{14}$$

where $\omega_\parallel$ corresponds to the trapping potential on the longitudinal axis. In our setup, the potential along z given in Eq. (1) is parabolic only in the vicinity of $z = 0$, but we can write $\omega_\parallel^2 \approx \frac{1}{m} [\partial_z^2 V(\vec{r})]_{x=y=z=0} = 2 \tilde{V}_0 \omega_\perp^2 / \tilde{L}^2$. By inserting the numerical values describing the initial conditions of the simulations of Figs. 1 and 6, we find $\delta_c^2 = 0.18$ and $\delta_c^2 = 0.23$, respectively. Assuming $N \approx N_0$ and, obviously $T < T_c$, we see that fluctuations are not large on any distance scale since $\delta_c^2 < 1$. This shows that for the situations we have analyzed this effect would not spoil an eventual interferometric measurement, even if it may reduce the contrast of the observable signatures. If in some other case one had $N \approx N_0$ but $\delta_c^2 \gg 1$, it would be necessary to cool down the condensate below $T_\phi = T_c / \delta_c^2$ [36] in order to avoid problems with this kind of phase fluctuation.

Finally, we would like to mention that soliton splitting in different situations has been investigated in a quantum framework beyond the mean-field GPE in Refs. [13,14,17].

[1] M. H. Anderson *et al.*, Science **269**, 198 (1995); K. B. Davis, M. O. Mewes, M. R. Andrews, N. J. vanDruten, D. S. Durfee, D. M. Kurn, and W. Ketterle, Phys. Rev. Lett. **75**, 3969 (1995).

[2] M. O. Mewes, M. R. Andrews, D. M. Kurn, D. S. Durfee, C. G. Townsend, and W. Ketterle, Phys. Rev. Lett. **78**, 582 (1997).

[3] A. D. Cronin, J. Schmiedmayer, and D. E. Pritchard, Rev. Mod. Phys. **81**, 1051 (2009).

[4] B. Lucke *et al.*, Science **334**, 773 (2011).

[5] A. Widera, O. Mandel, M. Greiner, S. Kreim, T. W. Hansch, and I. Bloch, Phys. Rev. Lett. **92**, 160406 (2004).

[6] S. Dimopoulos, P. W. Graham, J. M. Hogan, M. A. Kasevich, and S. Rajendran, Phys. Rev. D **78**, 122002 (2008).

[7] Y. Shin, M. Saba, T. A. Pasquini, W. Ketterle, D. E. Pritchard, and A. E. Leanhardt, Phys. Rev. Lett. **92**, 050405 (2004); T. Schumm *et al.*, Nat. Phys. **1**, 57 (2005).

[8] J. Chwedenczuk, P. Hyllus, F. Piazza, and A. Smerzi, arXiv:1108.2785 [quant-ph].

[9] C. Gross *et al.*, Nature (London) **464**, 1165 (2010).

[10] K. E. Strecker, G. B. Partridge, A. G. Truscott, and R. G. Hulet, Nature (London) **417**, 150 (2002).

[11] L. Khaykovich *et al.*, Science **296**, 1290 (2002).

[12] N. G. Parker, A. M. Martin, S. L. Cornish, and C. S. Adams, J. Phys. B **41**, 045303 (2008).

[13] C. Weiss and Y. Castin, Phys. Rev. Lett. **102**, 010403 (2009).

[14] A. I. Streltsov, O. E. Alon, and L. S. Cederbaum, Phys. Rev. A **80**, 043616 (2009).

[15] T. P. Billam, S. L. Cornish, and S. A. Gardiner, Phys. Rev. A **83**, 041602 (2011).

[16] U. Al Khawaja and H. T. C. Stoof, New J. Phys. **13**, 085003 (2011).

[17] A. D. Martin and J. Ruostekoski, New J. Phys. **14**, 043040 (2012).

[18] J. L. Helm, T. P. Billam, and S. A. Gardiner, Phys. Rev. A **85**, 053621 (2012).

[19] L. D. Carr and J. Brand, Phys. Rev. A **70**, 033607 (2004).

[20] H. Ott, J. Fortagh, G. Schlotterbeck, A. Grossmann, and C. Zimmermann, Phys. Rev. Lett. **87**, 230401 (2001); W. Hänsel, P. Hommelhoff, T. W. Hänsch, and J. Reichel, Nature (London) **413**, 498 (2001).

[21] S. Inouye *et al.*, Nature (London) **392**, 151 (1998).

[22] M. Theis, G. Thalhammer, K. Winkler, M. Hellwig, G. Ruff, R. Grimm, and J. H. Denschlag, Phys. Rev. Lett. **93**, 123001 (2004).

[23] L. D. Carr and J. Brand, Phys. Rev. Lett. **92**, 040401 (2004).

[24] D. M. Stamper-Kurn, M. R. Andrews, A. P. Chikkatur, S. Inouye, H. J. Miesner, J. Stenger, and W. Ketterle, Phys. Rev. Lett. **80**, 2027 (1998).

[25] J. P. Martikainen, Phys. Rev. A **63**, 043602 (2001).

[26] E. P. Gross, Nuovo Cimento **20**, 454 (1961); L. P. Pitaevskii, Sov. Phys. JETP-USSR **13**, 451 (1961); F. Dalfovo, S. Giorgini, L. P. Pitaevskii, and S. Stringari, Rev. Mod. Phys. **71**, 463 (1999).

[27] V. M. Pérez-Garcia, H. Michinel, and H. Herrero, Phys. Rev. A **57**, 3837 (1998).

[28] V. Ramesh Kumar, R. Radha, and P. K. Panigrahi, Phys. Lett. A **373**, 4381 (2009).

[29] M. A. de Moura, J. Phys. A **27**, 7157 (1994).

[30] V. M. Pérez-García, H. Michinel, J. I. Cirac, M. Lewenstein, and P. Zoller, Phys. Rev. Lett. **77**, 5320 (1996).

[31] V. I. Bespalov and V. I. Talanov, Zh. Eksp. Teor. Fiz. Pis'ma Red. (USSR) **3**, 471 (1966) [JETP Lett. **3**, 307 (1966)].

[32] M. I. Rodas-Verde, H. Michinel, and V. M. Pérez-García, Phys. Rev. Lett. **95**, 153903 (2005).

[33] T. P. Billam, S. A. Wrathmall, and S. A. Gardiner, Phys. Rev. A **85**, 013627 (2012).

[34] S. Sinha, A. Y. Cherny, D. Kovrizhin, and J. Brand, Phys. Rev. Lett. **96**, 030406 (2006).

[35] H. Buljan, M. Segev, and A. Vardi, Phys. Rev. Lett. **95**, 180401 (2005).

[36] D. S. Petrov, G. V. Shlyapnikov, and J. T. M. Walraven, Phys. Rev. Lett. **87**, 050404 (2001).

[37] D. S. Petrov, G. V. Shlyapnikov, and J. T. M. Walraven, Phys. Rev. Lett. **85**, 3745 (2000).